

Effects of Cortical Spreading Depression on Cortical Blood Flow, Impedance, DC Potential, and Infarct Size in a Rat Venous Infarct Model

H. Otsuka, K. Ueda, A. Heimann, and O. Kempfski¹

Institute for Neurosurgical Pathophysiology, Johannes Gutenberg University, 55101 Mainz, Germany

Received July 29, 1999; accepted November 15, 1999

A cortical venous infarction model has been evaluated as to the degree of regional flow reduction and by studying effects of cortical spreading depression (CSD). Two adjacent cortical veins were occluded photochemically with rose bengal and fiberoptic illumination. Seven rats served to demonstrate effects on regional cortical blood flow using laser Doppler scanning. In 36 rats local CBF, DC potential, and brain tissue impedance were measured continuously for 75 min after vein occlusion. No, 3, or 10 CSD waves were induced by potassium chloride injection during the initial 75 min. Rats were compared for spontaneous CSDs; baseline local CBF, CBF, and impedance response to CSD; and infarct volume. Seventy-five minutes after vein occlusion regional cortical flow in a 3.5 × 7-mm window was reduced to 34.3 ± 13.2%. At 45% of the 840 measured locations in 7 rats flow was <40% baseline and at 27.3% <30%, indicating a widespread penumbra territory. During the initial 75 min 2.1 ± 1.1 spontaneous CSDs were observed. There was a positive correlation between the number of spontaneous CSDs seen acutely and infarction volume after 5 days. Moreover, brain injury was significantly increased in the group with 10 KCl-induced CSDs. A reduced lCBF response and an overshooting tissue impedance change during CSD were predictors of ischemic damage. This study demonstrates a CSD-related growth of the venous infarct. Second, the data indicate that flow after two-vein occlusion resembles that seen under penumbra conditions, allowing for studies of damage mechanisms responsible for infarct growth. © 2000 Academic Press

Key Words: spreading depression; cerebral blood flow; venous infarct; laser Doppler flowmetry; photochemical thrombotic technique; impedance; penumbra; rat

INTRODUCTION

Focal cerebral ischemia due to venous obstruction has long been considered a rare event compared to arterial ischemia. Better diagnostic tools such as magnetic resonance tomography indicate that sinus-vein thrombosis is not that uncommon (28). Invasive neurosurgical interventions, moreover, often require the ligation of cerebral veins. Therefore, a detailed understanding of the pathophysiology of venous ischemia is necessary. During recent years rat models have been developed for that purpose (20–24): The occlusion of two adjacent cortical veins is followed by a reduced regional CBF (rCBF) and by the occurrence of comparatively small infarcts (9, 20), whereas occlusion of solitary veins causes reduction of cortical blood flow without reproducible infarct development (20, 23). Although CBF data available for the two-vein occlusion model suggest a rather widespread reduction of CBF (20, 23) it remained unclear so far whether this flow reduction is similar to that encountered in arterial penumbra zones. The comparatively small infarct volume makes the two-vein occlusion model particularly suited to study pathophysiological mechanisms responsible for the secondary growth of an infarct, i.e., mediator mechanisms such as cortical spreading depression (CSD), which are thought to contribute to the decay of arterial penumbra zones (11). CSD has not been studied in venous ischemia so far. The current study, therefore, had two aims: (a) to critically evaluate the degree of regional cortical flow reduction after two-vein occlusion and (b) to test whether CSDs—occurring during the acute phase either spontaneously or induced by microinjection of isotonic KCl—similar to arterial infarcts can cause the development of larger infarcts after 5 days.

MATERIALS AND METHODS

This study was conducted according to the German animal protection legislation and has been reviewed by the regional ethics committee (Bezirksregierung Rheinland-Pfalz).

¹To whom correspondence and reprint requests should be addressed at the Institute for Neurosurgical Pathophysiology, Johannes Gutenberg University, 55101 Mainz, Germany. Fax: +49-6131-176640. E-mail: kempfski@nc-patho.klinik.uni-mainz.de.

Animal Preparation

The experiments were carried out in 37 male Wistar rats (302 ± 26 g, range 255–350 g body weight; Charles River, Germany). The animals were housed in individual cages and allowed free access to food and water before and after surgery. Animals were anesthetized by ether and intraperitoneal injection of chloral hydrate (36 mg/100 g body wt) after premedication with 1.0 mg atropine. Anesthesia was maintained by chloral hydrate (12 mg/100 g body wt) given hourly through a peritoneal catheter. In all animals, the trachea was intubated with silicon tube (o.d. 2.5 mm), and animals were mechanically ventilated with 30% oxygen using a rodent ventilator (Model 683; Harvard Apparatus, South Natick, MA) under control of end expiratory PCO_2 (Artema MM206C; Heyer, Sweden). Rectal temperature was kept close to 37.0°C throughout the experiment by a feedback-controlled heating pad (Harvard Apparatus). Polyethylene catheters (o.d. 0.96 mm, Portex; A Smiths Industries Medical Systems Co., UK) were inserted into the right femoral artery and vein. The arterial line served for continuous registration of mean arterial blood pressure (MABP) and arterial blood gas sampling and the venous lines for administration of fluid and drugs. P_aO_2 , P_aCO_2 , arterial pH, and electrolytes were measured with a blood gas and electrolyte analyzer (ABL System 615; Radiometer, Copenhagen, Denmark). Blood pressure was continuously monitored through the intra-arterial catheter connected to a pressure transducer (Gould 134615-50). Rats were mounted in a stereotaxic frame (Stoelting, Wood Dale, IL). After a 2.0-cm midline skin incision, a right frontoparietal cranial window was made for access to the brain surface using a high-speed drill under an operating microscope (OP-Microscope, Zeiss, Wetzlar, Germany). During the craniectomy, the drill tip was cooled continuously with physiologic saline to avoid thermal injury to the cortex. The dura was left intact.

Cortical Vein Occlusion by Photochemical Thrombosis

The occlusion of two adjacent cortical veins was induced using rose bengal dye (Sigma, St. Louis, MO) and fiberoptic illumination using a 50-W mercury lamp (6500–7500 lx, 540 nm) connected to a 100- μm fiber (20, 21, 23). Only animals with a similar venous anatomy were used, i.e., with two prominent adjacent veins connecting into the superior sagittal sinus (cf. Fig. 1B). The diameter of the occluded veins was approximately 100 μm . Rose bengal (50 mg/kg body wt) was injected slowly without effect on the systemic arterial pressure, and care was taken to avoid illumination of tissue and other vessels near the target vein. The vein was illuminated for 10 min via the micromanipulator-assisted light guide. To occlude the second selected vein, half of the initial rose bengal dose was injected

intravenously before the illumination was repeated with the new target.

Experimental Groups

Seven rats were used to study local cortical blood flow using laser Doppler scanning (group S). The effects of CSD on local CBF, DC potential, impedance, and histological outcome were assessed in groups A, B, and C. In group A ($n = 10$) the occurrence of spontaneous CSD was monitored for 75 min. Animals from group B received three cortical microinjections of KCl in 21-min intervals ($n = 12$), whereas 10 microinjections in 7-min intervals were performed in group C ($n = 14$).

Measurement of CBF Using LD Flowmetry

Local CBF was measured by laser Doppler (Model BPM 403a; Vasomedics, St. Paul, MN) with 0.8-mm needle probes. Flow is expressed in LD units, which are not arbitrary but have a low biological zero (0–1 LD units) and are one-point calibrated with latex beads at 25°C in a Teflon vial. We have previously been able to show that laser Doppler readings correlate linearly with hydrogen clearance provided that several adjacent cortical locations are scanned by laser Doppler (29) to overcome the high spatial variability of local flow measurements.

One experimental series (group S) was performed to study the regional reduction of local CBF after two-vein occlusion. To do so, the cortical CBF pattern was mapped in seven rats with the dura remaining intact. Local CBF was measured at 120 (8×15) locations with the occluded veins lateral to the scanning field (3.5×7.0 mm) using a stepping-motor-driven and computer-controlled micromanipulator (10, 21, 23). Thus, one scanning procedure yielded information from 120 different locations each at a distance of 500 μm . Measurements from individual locations are referred to as local CBF (lCBF), the median of the 120 lCBF values from individual rats is termed regional CBF. The technique permits repeated scans for a given set of locations. Scanning was performed from the beginning to the end of the experiment at identical locations at 15-min intervals. Data were also used to create flow maps and to establish observation frequency histograms. The median of observation frequency histograms correlates with absolute blood flow as determined by hydrogen clearance (29).

In all other 36 experiments (groups A, B, and C) lCBF was measured at two stationary locations. The first LD probe (LD probe 1) was placed centrally between the two occluded veins (Fig. 1). The second LD probe (LD probe 2) was placed outside the two occluded veins on the lateral frontal cortex. Both probes were positioned close to the dura surface, avoiding visible vessels. Only locations with a baseline flow of 30–45 LD units were accepted.

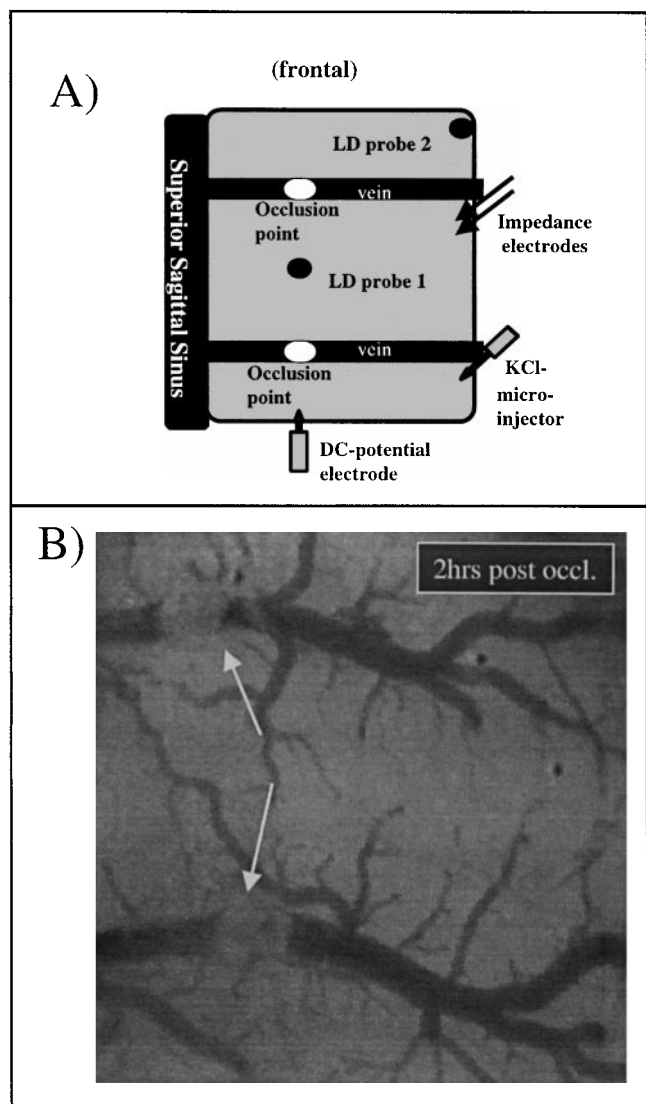


FIG. 1. Schematic drawing of the experimental setup (A) and video image of a typical experiment 75 min after vein occlusion. (A) The locations of all electrodes and the occlusion sites of two adjacent cortical veins of the parietal cortex are indicated. Electrodes, KCl microinjector, and LD probes were placed to ensure that distances between KCl injector and DC potential electrode, impedance electrode, and LD probe 1 were comparable. (B) Video image as observed through the closed dura 75 min after vein occlusion. Arrows indicate locations of the thrombi. Before and behind the thrombi, veins exhibit stasis or flow reversal, which, however, can be visualized only by fluorescence angiography (21, 23).

DC Potential and Impedance Measurement

The DC-potential electrode was made of glass tube (GB150F-10; Science Products GmbH, Hofheim, Germany) using a micropipette puller (Flaming/Brown Model P-97; Sutter Instrument, U.S.A.). The glass micropipette, after being filled with 0.9% NaCl and insertion of a silver/silver chloride wire, was impaled into the cortex (0.2–0.4 mm depth). The potential

between this electrode and an Ag/AgCl electrode placed in the neck muscle was recorded during the experiment. For grounding the stereotaxic frame was used. The signal was fed to a DC amplifier (Gould, Inc., Cleveland, OH) and recorded on a chart recorder (BBC, Goerz Metrawatt, Germany). Ten minutes of a stable potential was allowed after DC-potential electrode insertion, before the two impedance electrodes were introduced into the cortex (0.4–0.5 mm depth, distance 3 mm, Fig. 1). The impedance electrodes were made from two stainless steel wires (o.d. 0.5 mm) covered by polyvinyl chloride for electrical insulation except for the 0.3-mm sharp-pointed tip. Impedance was measured at 1 kHz (10 mV, bias-free) throughout the experiment using a precision LCR monitor (4284A; Hewlett–Packard, U.S.A.).

Induction of Cortical Spreading Depression

Ten minutes after impedance electrode insertion, the KCl injector, a glass micropipette filled with 150 mmol/L KCl solution, was inserted into the lateral parietal cortex (Fig. 1). It was connected to a microinjection pump (CMA/100; Carnegie Medicine, Stockholm, Sweden). In Groups B and C, rats received 3 or 10 KCl injections (2.0 μ l) into the parietal cortex beginning after completion of the two-vein occlusion and ending 75 min thereafter. Rats in group A were not injected with KCl. Electrodes and LD probe 1 were placed at equal distances to the KCl injector (Fig. 1).

Histological Preparation

After operation the skin wounds were closed with 4-0 silk. The rats were returned to individual cages and allowed free access to water and food. Body weight of all rats was measured every morning until the fifth day after operation. Then, the rats were perfusion-fixed with 4% paraformaldehyde after general anesthesia with chloral hydrate. Then, the brain was removed from the skull carefully. Brains were embedded in paraffin to obtain coronal sections of the parietal region. Sections were stained with hematoxylin/eosin and luxol fast blue. The histological evaluation was performed by light microscopy. A CCD camera (Sony, Tokyo, Japan) and a Maxigen Genlock interface (Merkens EDV, Bad Schwabach, Germany) were used to project microscopic images onto the screen of an Amiga 2000 computer (Commodore, Braunschweig, Germany). For quantitative assessment of brain injury, infarct size was measured in 34 sections using software developed in this laboratory. The infarcted area was evaluated in serial sections in 90- μ m steps. The infarction volume V_1 was calculated from infarct areas A_n in 34 sections and the distance between sections ($d =$

90 μm) according to the formula

$$V_I = \sum A_n \times d.$$

The image analysis system was calibrated with a microscope ruler (Ernst Leitz, Wetzlar, Germany).

Statistical Analysis

Data are expressed as means \pm standard deviation. Sequential changes within the groups were statistically evaluated by ANOVA (Dunnett's test) for repeated measures. The Kruskal–Wallis test with multiple comparisons was used to study differences between groups (Sigma-Stat; Jandel Scientific, Erkrath, Germany). Statistical significance was assumed at an error probability of $P < 0.05$. Flow contour maps were created from the 120 scanning data using Sigma-Plot (Jandel Scientific).

RESULTS

Physiological Variables

There were no statistical differences in blood gases ($P_a\text{O}_2$, $P_a\text{CO}_2$, and pH) or electrolytes (Na^+ and K^+) before and after cortical vein occlusion or among the groups. MABP was not significantly changed by vein occlusion or CSD induction with KCl and remained between 85 and 100 mm Hg throughout the study in all groups.

Cortical CBF Mapping

Cortical ICBF mapping revealed a typical pattern of local flow values (Fig. 2A). The observation frequency histogram at baseline has two peaks, with ICBF < 60 LD units typical for the microcirculation and larger values from the vicinity of veins and arteries. ICBF readings < 15 LD units are found at only 4.2% of locations. The median of the total population of 840 scanned locations in seven rats was 47.09 LD units. Averaging the median ICBF values of individual rats yields 50.13 ± 7.78 LD units, which may serve as an estimate of regional CBF in the affected cortex. Seventy-five minutes after venous occlusion a widespread rCBF reduction down to 16.98 ± 6.40 LD units ($=34.32 \pm 13.2\%$) had occurred (Fig. 2B). Local CBF was < 15 LD units in 41.9% of the 840 locations. In 45% of these locations ICBF was below 40% of baseline flow, in 27.8% below 30% baseline flow, and in 15% below 20% baseline flow (Fig. 2C). An example of flow maps taken at baseline and 75 min after two-vein occlusion from an individual rat is given in Fig. 3. In this animal rCBF decreased from 56.8 to 18.1 LD units. How this regional effect translates into local flow changes is indicated in

Fig. 3, bottom, in which all local flow changes are expressed on a percentage scale.

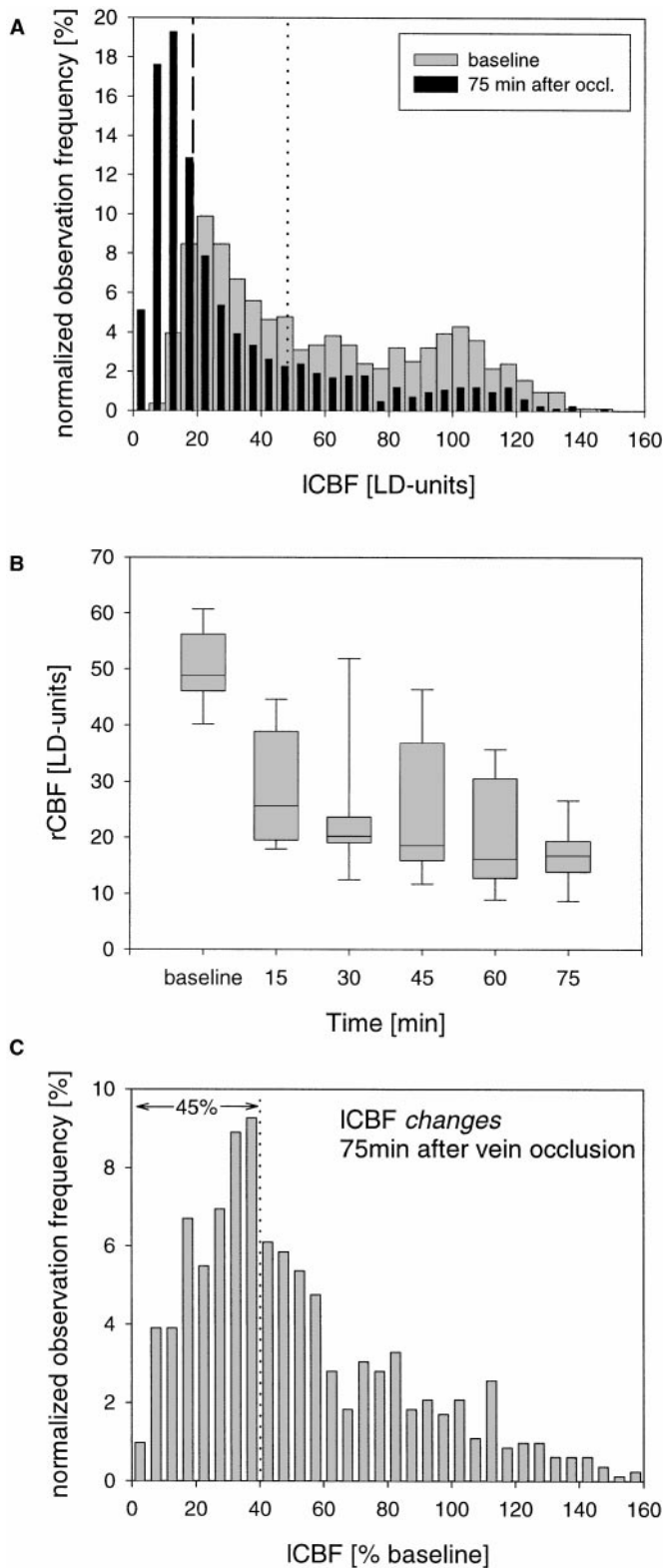
DC Potential, Impedance, and Local CBF Changes after CSD

DC potential as well as cortical impedance was stable under baseline conditions in all tested rats. Within 60–120 s after KCl injection into the cortex, a solitary episode of CSD was always observed for 60–180 s as negative deflection of the DC potential and a temporary increase of tissue impedance and ICBF (Fig. 4). In addition, spontaneous CSD waves were observed zero to four times during the initial 75 min after cortical two-vein occlusion (Fig. 4). DC potential and impedance always normalized after CSD, a terminal depolarization-like alteration of DC potential or impedance was never observed. In a parallel series of experiments in which one episode of CSD was induced in 18 sham-operated animals it was verified that KCl injection never triggers more than one single CSD wave (data not shown).

Baseline ICBF was well comparable in the three experimental groups A, B, and C (Fig. 5A). Related to the individual vascular anatomy under the flow probes, baseline flow measured at LD probe 1 (between the occluded veins) was moderately lower than that seen at probe 2. After photothrombosis there was a ICBF reduction (cf. Fig. 2B), which in most animals became more severe during the 75-min observation period (Table 1). The aggravation of the flow reduction reached statistical significance in group C only (Table 1). The average increase of ICBF during CSD registered with LD probe 1 between the two occluded veins was minimal compared to that seen at LD probe 2, i.e., outside the occluded veins (Fig. 5). In group C (10 induced CSD waves) the flow increase during CSD was significantly smaller than in group A also at LD probe 2 (outside the two occluded veins) (Fig. 5B). In most cases ICBF between the occluded veins decreased gradually over time. A typical example is shown in Fig. 4. Interestingly, local flow often decreased after a CSD wave had passed (Fig. 4).

Infarct Volume

All rats studied had a cortical infarct. In group A (no CSD induction), all rats had parenchymal damage surrounding dilated capillaries and edematous areas in white and gray matter. Rats in groups B and C showed more extensive infarction. Quantitative assessment of brain injury yielded a significantly larger infarct size in group C (10.5 ± 4.9 mm^3 , $n = 11$) than in group A (3.6 ± 2.2 mm^3 , $n = 10$) ($P < 0.001$). In group B, though infarct volume tended to be larger (6.8 ± 4.7 mm^3 , $n = 10$) than in group A, differences did not reach statistical significance (Fig. 6).



Relationship between Spontaneous CSD and Infarct Volume

After cortical two-vein occlusion, spontaneous CSDs were observed 2.1 ± 1.1 times (range 0–4 times) during the initial 75 min, i.e., the acute phase of the experiment. There were no significant differences in the number of spontaneous CSD waves observed during that time among the groups. There were, however, positive correlations between the number of spontaneous CSDs and infarct volume in the groups: the correlation coefficients were 0.876 in group C ($P < 0.001$), 0.833 in group B ($P = 0.004$), and 0.857 in group A ($P = 0.005$; Fig. 7). The second order polynomial regression lines of groups A and B were virtually identical (Fig. 7), only that of group C with 10 KCl-induced CSDs was shifted upward toward larger infarct volumes: at identical numbers of spontaneous CSDs infarct volumes were nearly doubled compared to groups A and B (Fig. 7).

Local CBF, Impedance, and Infarct Volume

Baseline ICBF between the two target veins before occlusion showed no significant difference among groups (Fig. 5A) nor was there any group difference after photothrombosis (Table 1). After two-vein occlusion ICBF declined significantly beginning at 15 min after occlusion ($P < 0.05$) in all groups. A plot of ICBF measured at LD probe 1 at the end of the acute phase of the experiment (after 75 min) versus infarct volume determined after 5 days reveals a threshold of 12–15 LD units below which infarction volume increased dramatically (Fig. 8). Dividing all rats into two subgroups with a threshold ICBF of 15 LD units 75 min after vein occlusion, there is a significantly larger infarction size in the subgroup with $ICBF \leq 15$ LD units (10.6 ± 4.6 mm³, $n = 15$) than in the subgroup

FIG. 2. Changes of ICBF and rCBF after two-vein occlusion in group S. Since laser Doppler measurements reflect local flow only, regional perfusion was evaluated by scanning 120 localizations in each rat. (A) Normalized observation frequencies were calculated of all ICBF data collected at 840 locations in 7 rats before (baseline) and 75 min after vein occlusion. By doing so, the median value of the histogram reflects regional flow and was found at 47.09 LD units at baseline (indicated by the dotted line), whereas median flow 75 min after occlusion was 18.2 LD units only (dashed line). The observation frequency histograms are characterized by two peaks, one representing readings from the microcirculation and the other from regions in the vicinity of large vessels. After vein occlusion the histogram shifts to the left toward lower values. (B) Changes of regional CBF (obtained from averaging median ICBF data of individual rats); there was typically more than 50% reduction of rCBF 75 min after occlusion. (C) The computerized scanning of the 840 location permits to evaluate flow changes at each location. The observation frequency histogram of flow changes reveals that 75 min after vein occlusion blood flow had decreased below 40% of baseline ICBF (indicated by dotted line) at 45% of all locations.

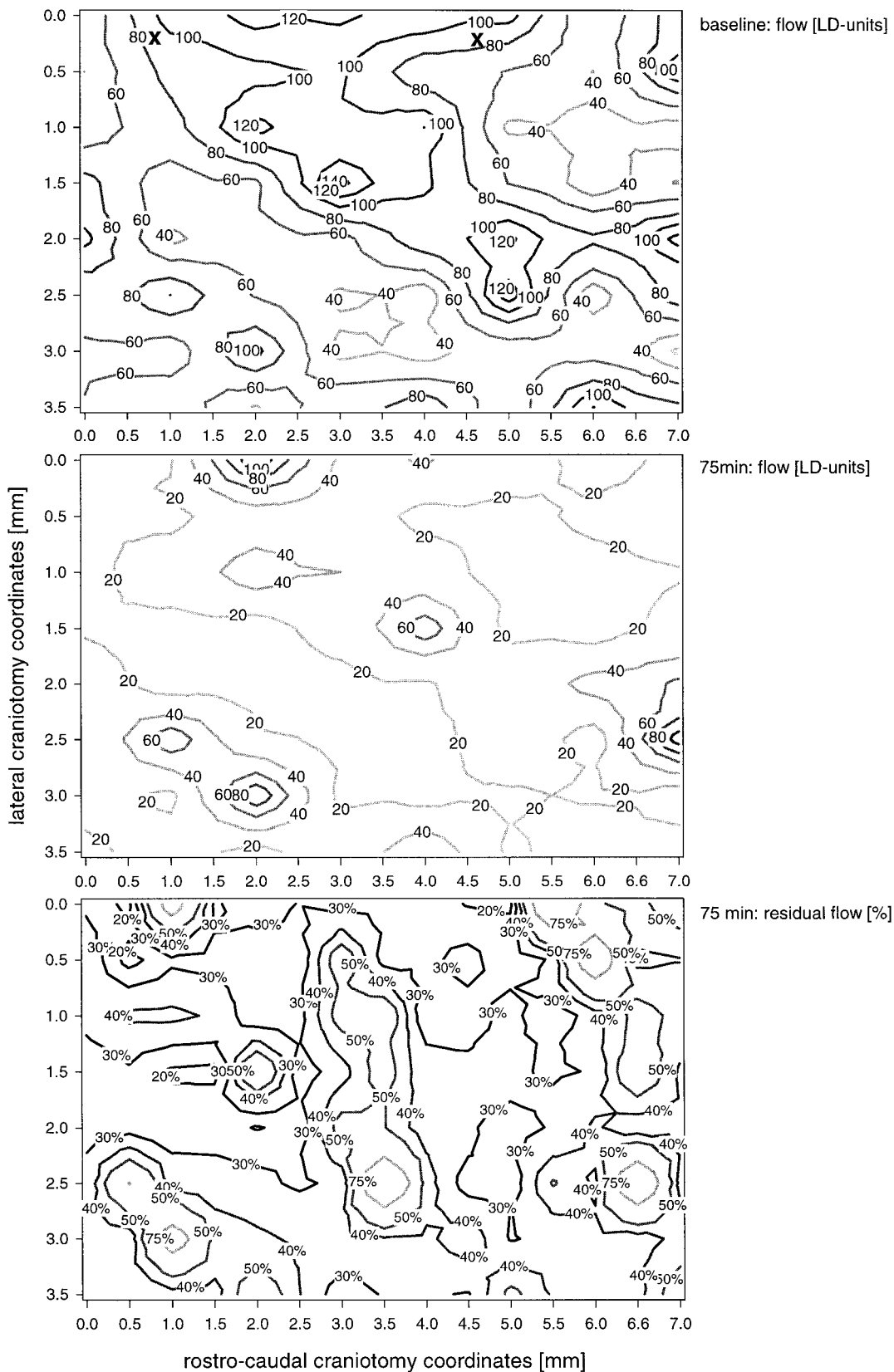


FIG. 3. Flow maps of an individual animal from group S calculated from the ICBF values found at 120 locations (3.5×7 -mm scanning field) at baseline (top) and 75 min after two-vein occlusion (middle). The calculation of flow changes (% baseline flow) for each location (bottom) reveals a rather heterogeneous pattern with vast areas of flow reduction below 40% baseline. Regions with complete ischemia (ICBF < 10%) are practically absent at this early stage. Therefore, in the early phase of this venous infarction model low-flow areas are far more common than areas with no flow at all.

with ICBF > 15 LD units (3.8 ± 1.9 mm³, $n = 16$) ($P < 0.001$).

The significance of the residual flow after vein occlusion for outcome is also illustrated by the flow change during CSD. Largest infarcts were found in animals in which CSD could elicit only small ICBF responses (< 10 LD units $\sim 30\%$ of flow before CSD) compared to those with large responses which had small infarcts (Fig. 9).

Brain-tissue impedance increased temporarily in all rats during CSD. Brain-tissue impedance was further evaluated by averaging the impedance maximum reached during individual CSD episodes: animals with larger impedance values during CSD had more severe brain damage (Fig. 10).

DISCUSSION

The data demonstrate that the occlusion of two cortical veins is accompanied by a circumscribed reduction of cortical flow to critical levels, which, however, do not reach levels typically encountered in global cerebral ischemia using similar methodology (27), i.e., below 10 LD units. Although initially flow readings typical of an ischemic core (< 10 LD units) are virtually absent, after 5 days an infarct of reproducible volume is regularly found. There is, hence, a gradual deterioration of flow, which during the 75 min of observation dropped to a critical level between 20 and 15 LD units at nearly 50% of all measured locations (Fig. 2C) and which finally after 5 days has caused structural damage and infarction. These conditions bear resemblance to those encountered in the vicinity of arterial infarcts, i.e., the ischemic penumbra.

The ischemic penumbra was initially characterized as tissue in the close neighborhood of an ischemic core with flow between two thresholds, the upper threshold of electrical failure and the lower of energy failure and ion pump failure (1). The penumbra has also been described by electrical silence with normal or slightly elevated extracellular potassium concentrations (1). Meanwhile a more complex pattern of thresholds has been suggested (10): at declining flow rates protein synthesis is inhibited first, followed by stimulation of anaerobic glycolysis, the release of neurotransmitters, the beginning disturbance of energy metabolism, and, finally, anoxic depolarization at ICBF < 0.15 ml/g/min. No matter which definition is applied, the fate of the ischemic penumbra contributes significantly to outcome of stroke. The fate of the penumbra may modify the degree of damage but certainly many other factors including the size of the core and its location are also important. Without treatment the conditions in the penumbra tend to deteriorate, and the ischemic core expands. The pathophysiological mechanisms involved in secondary damage to penumbra tissue are currently studied in rat models with occlusion of the middle

cerebral artery, in which the ratio core:penumbra increases rapidly from approx 1:1 to 10–20:1 within 4–6 h (7). The relationship between the type of damage produced by venous occlusion versus arterial occlusion requires further study.

Two-Vein Occlusion as a Model of the Ischemic Penumbra

The thrombosis of a solitary vein goes along with a rather widespread reduction of microcirculatory flow and has been proposed as a penumbra model (21). One vein occlusion, however, does not necessarily cause infarcts (20). The two-vein occlusion model may present a promising alternative to study the pathophysiology of a peri-ischemic low-flow zone. It goes along with a rather widespread reduction of cortical flow (20, 23) (Fig. 3) and the development of infarcts of 2–5 mm³ infarct volume, i.e., $\sim 1/30$ the size of infarcts developing after middle cerebral artery (MCA) occlusion (7). Moreover, the kinetics of flow reduction and, hence, infarct development are slower than in arterial infarction (23). CBF mapping shows that low-flow areas cover a wide area, whereas the ischemic core is hardly detectable in the acute phase (cf. Fig. 3). ICBF was well comparable in individual rats under baseline conditions (Fig. 5) using laser Doppler flowmeters with a stable and low biological zero and a one-point calibration. The presence of penumbra conditions can be deduced from the rCBF decrease to 34.3% in the affected territory, which is also seen at the solitary locations measured in groups A, B, and C (Table 1). At selected locations ICBF increased above the baseline value after vein occlusion (Fig. 2C). This is due to the occurrence of flow reversal and the opening of collateral pathways which are often perfused with desaturated blood (22). Presence of penumbra conditions is furthermore suggested by the observed ~ 60 – 70% reduction of the ICBF response to CSD (Figs. 5 and 9), proving a compromised reserve capacity. In group C the ICBF stimulation by CSD was even impaired at LD probe 2 outside the two occluded veins as an indication that the massive metabolic demands by 10 induced CSD waves compromised surrounding tissues and caused a spread of penumbra conditions which then resulted in the growth of the ischemic core in that group.

Peri-infarct Depolarizations as Mediators of Damage to the Penumbra

There is now agreement that mediators activated or released from an ischemic core may negatively affect surrounding tissues with critically reduced flow. Peri-infarct depolarizations are discussed in this context, i.e., spreading depression waves triggered by the anoxic release of potassium and neurotransmitters in the infarct core, which are propagated over the whole

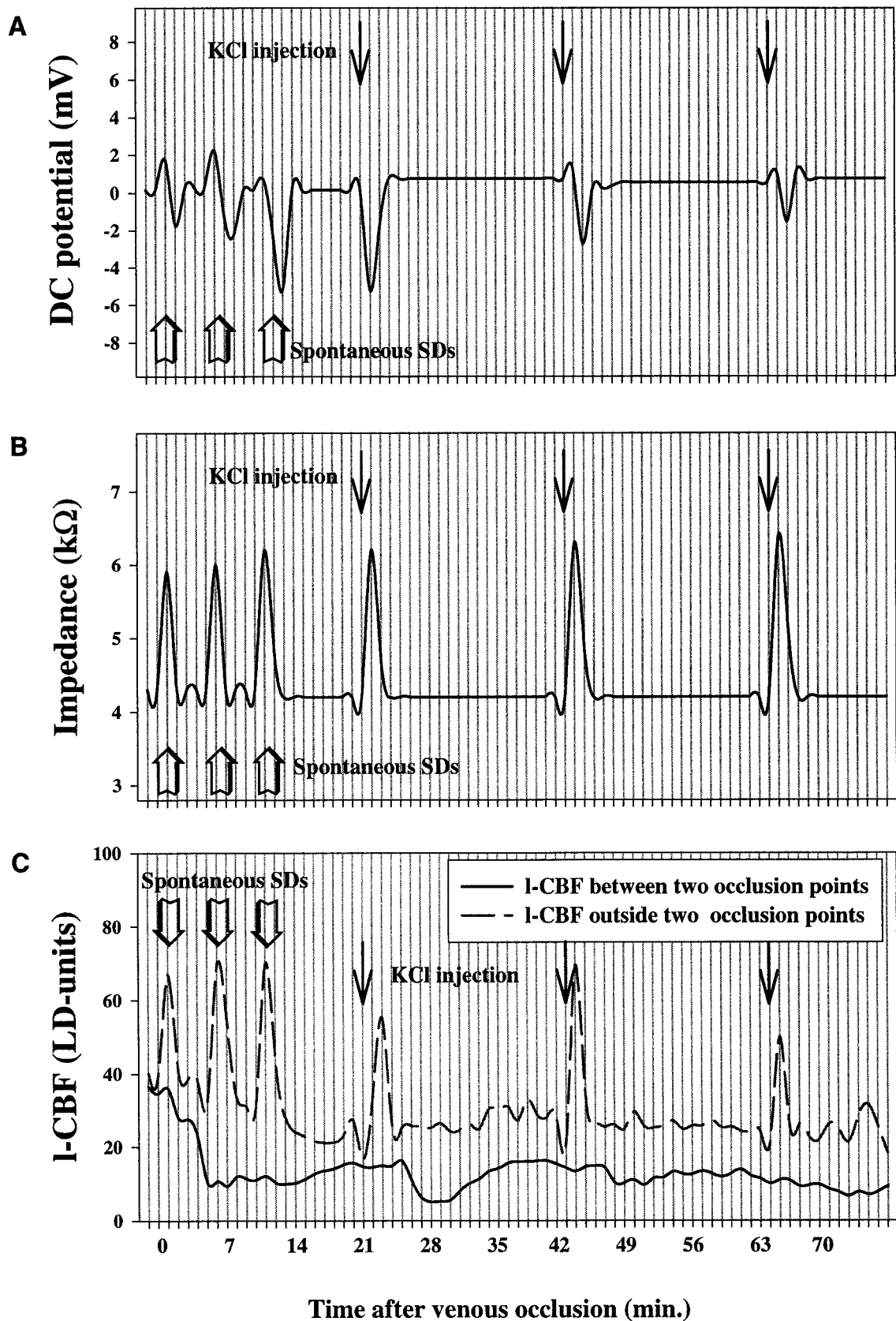


FIG. 4. Original recordings from a representative experiment with three KCl-induced CSDs. The graphs show sequential changes of DC potential (A), cerebral tissue impedance (B), and I-CBF (C). Line arrows indicate KCl injections (21st, 42nd, and 63rd min after venous occlusion), open arrows mark spontaneous spreading depression. Spontaneous CSDs were seen at random time points during the 75-min

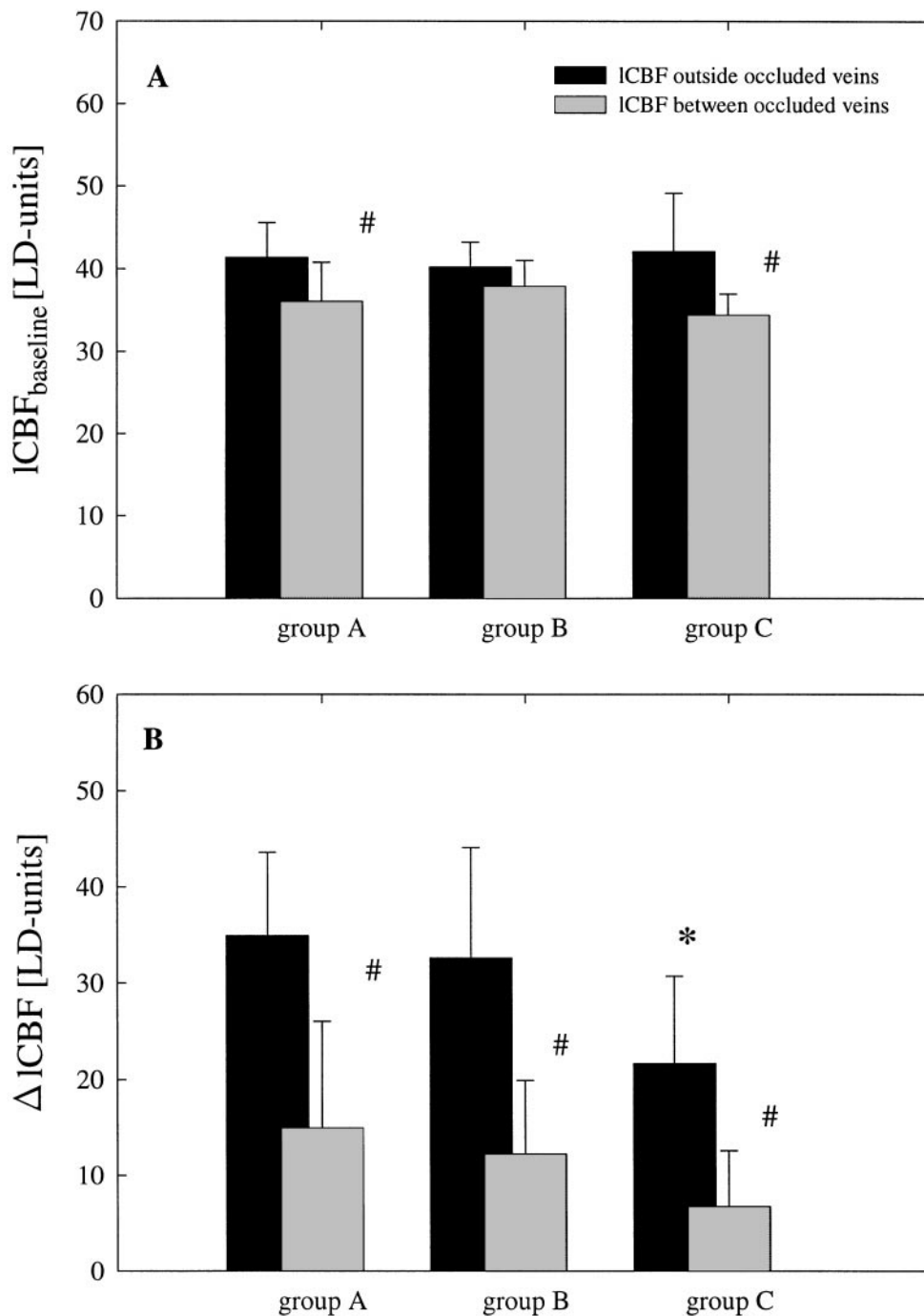


FIG. 5. Local CBF under baseline conditions (A) and flow increases during spreading depression (B) in the three experimental groups as measured at LD probes 1 (between occluded veins) and 2 (outside occluded veins). As a consequence of the underlying vascular anatomy, ICBF at LD probe 1 was somewhat lower under baseline conditions in all three groups. The flow increase during spreading depression was significantly reduced between the occluded veins ($\#P < 0.05$ vs LD probe 2). In group C the flow increase during CSD was also reduced at LD probe 2 outside the occluded veins ($*P < 0.05$ vs group A (no CSD induction)).

observation time. In the experiment shown here they all occurred during the initial 15 min. In this animal ICBF between the occlusion points did not increase during CSD. However, there was a typical reduction of ICBF at this measuring location after spontaneous as well as induced CSD. Outside the low-flow zone (at LD probe 2) there was the normal temporary CBF increase during CSD.

TABLE 1

Laser Doppler Flow (LD Units) Recorded at LD Probe 1 (between the Occluded Veins) at Baseline and 15, 45, and 75 min after Induction of Photothrombosis in Three Groups without or with 3 or 10 Induced CSD Waves during the Initial 75 min of the Experiment

	Group A (no CSD induction)	Group B (3 KCl- induced CSD)	Group C (10 KCl- induced CSD)
Baseline	36.07 ± 4.67	37.86 ± 3.14	34.38 ± 2.58
15 min vein occl.	25.51 ± 11.04	24.41 ± 8.18	21.77 ± 7.48
45 min vein occl.	21.89 ± 10.46	19.97 ± 5.56	15.95 ± 3.83*
75 min vein occl.	21.93 ± 11.89	18.72 ± 7.80	15.53 ± 6.51*

Note. Photothrombosis caused significant flow reduction in all groups (not indicated). Flow reduction deteriorated significantly in group C only (* $P < 0.05$ vs 15 min vein occl.).

hemisphere at a speed of ~ 3 mm/min (11). Since CSD was originally reported by Leão *et al.* (15) in 1944, the knowledge about this phenomenon has grown only slowly. The first systematic study on the involvement of CSD in the pathophysiology of arterial ischemia is that of Nedergaard and Astrup (1), who used the rat MCA occlusion model. The authors found peri-infarct CSD characterized by longer duration and spontaneous generation compared to CSD in normal tissue. More detailed analyses revealed a pathogenetic role of CSD

during the incorporation of the penumbra into the ischemic core: There is a correlation between the number of CSD waves and infarct volume (2, 19), and prevention of CSD by treatment with glutamate antagonists reduced infarct size (6). On the other hand CSD in normal brain is not associated with neuronal injury (26). Preconditioning with CSD has even been used to reduce infarct volume from MCA occlusion, making use of the metabolic stress evoked by CSD (16).

It has been reported that glucose consumption was increased threefold by CSD (8), that oxygen consumption showed a 45% increase during CSD passage, and that this rise is coupled to augmentation of flow and oxygen transport (17). Furthermore, cortical ATP concentration was significantly reduced during CSD (14, 18). Thus, CSD is an energy-requiring process that leads to substantial activation of energy metabolism (2). It is well accepted that CSD goes along with a temporary breakdown of ion gradients, and, thereafter, a massive increase of the cerebral metabolic rate which is blamed for the detrimental effect on the ischemic penumbra (11). CSD will further compromise the metabolic condition of the penumbra which is at a threshold from functional to structural damage (1).

Our findings confirm for venous infarcts that with an increasing frequency of CSD waves, infarct volume tends to increase considerably (2, 18). With 4 spontaneous peri-infarct depolarizations during the initial 75 min there was a more than threefold growth of the

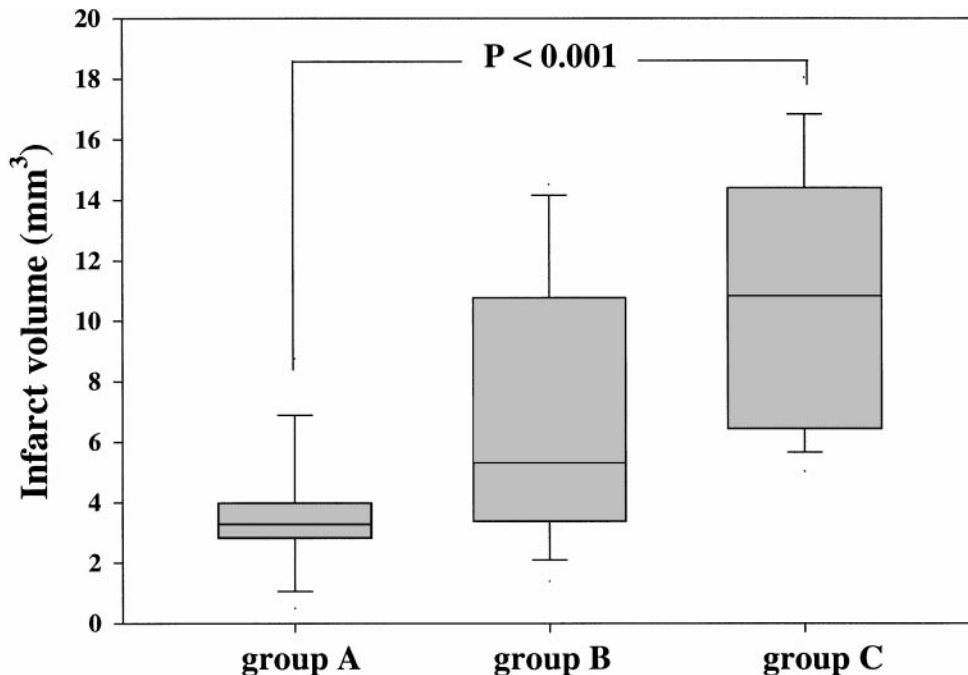


FIG. 6. Box plot showing results of quantitative assessment of infarct volume (mm^3) in the three experimental groups. Solid lines in each box show median value. Error bars indicate 5 and 95% percentile. Infarction volume was significantly larger in group C than in group A ($P < 0.05$).

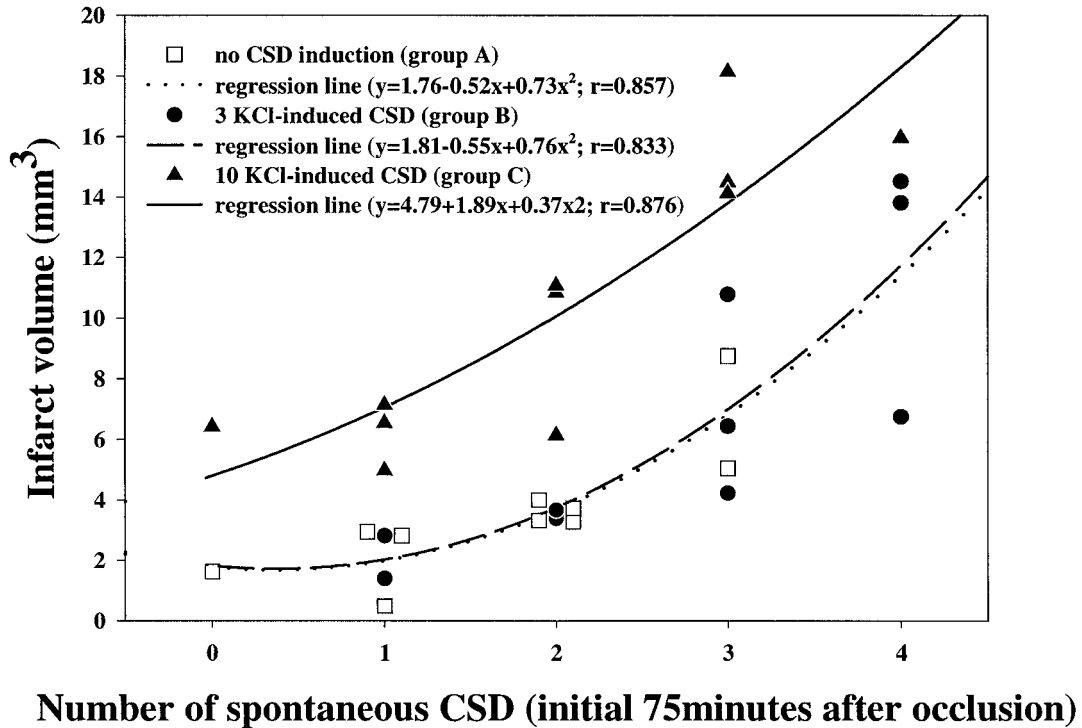


FIG. 7. Correlation between number of spontaneous CSDs and infarction volume of individual animals in groups without CSD induction, 3 KCl-induced CSDs, and 10 KCl-induced CSDs. Infarction volume was larger with growing number of spontaneous CSDs in each group. Note the nearly identical regression lines for groups A and B, whereas the regression line for group C is shifted upward toward larger volumes.

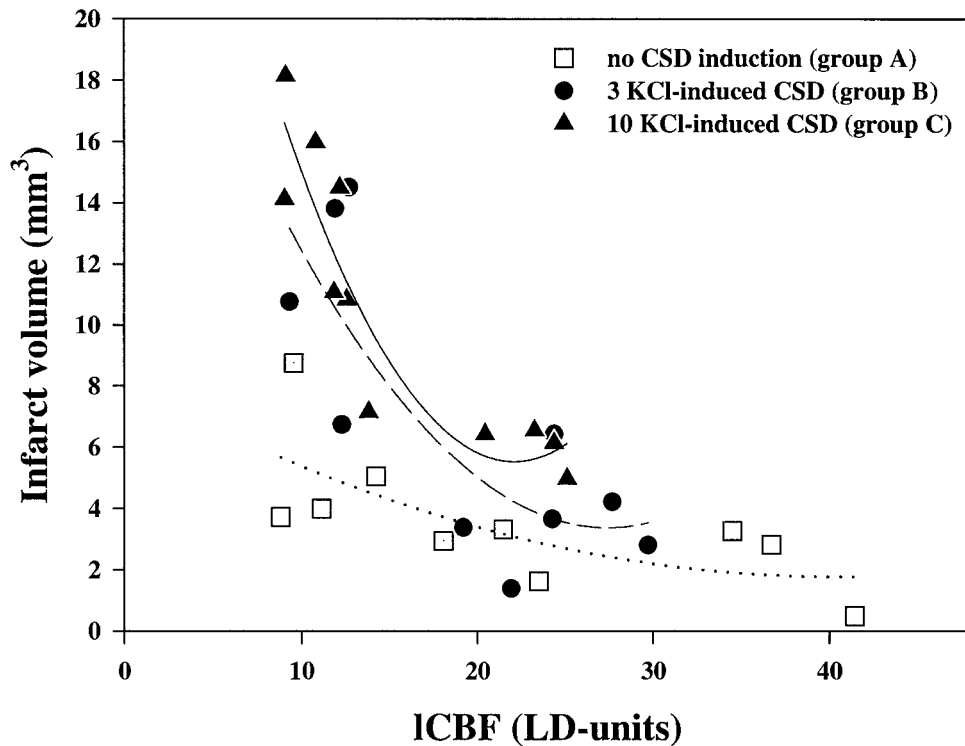


FIG. 8. The relationship between ICBF as measured 75 min after venous occlusion and infarct volume determined after 5 days in animals from the groups without CSD induction, i.e., with spontaneous CSDs only, 3 KCl-induced CSDs, and 10 KCl-induced CSDs. Symbols represent individual experiments. Infarct volumes were increased in animals with ICBF <12–15 LD units.

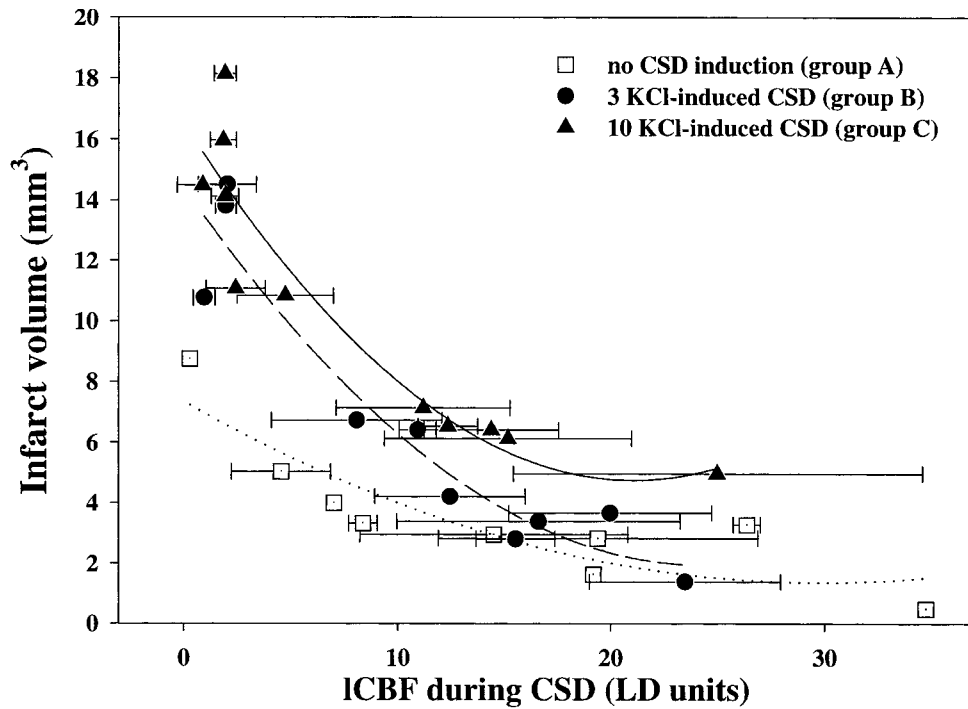


FIG. 9. Correlation of CSD-induced CBF increases and resulting infarct volumes in groups without CSD induction, with 3 KCl-induced CSDs, and with 10 KCl-induced CSDs. ICBF change is expressed in LD units (means \pm SD). Each data point shows the average of CBF responses during CSDs of an individual animal (\pm SD). Infarct volumes were larger in animals with a reduced CBF reaction.

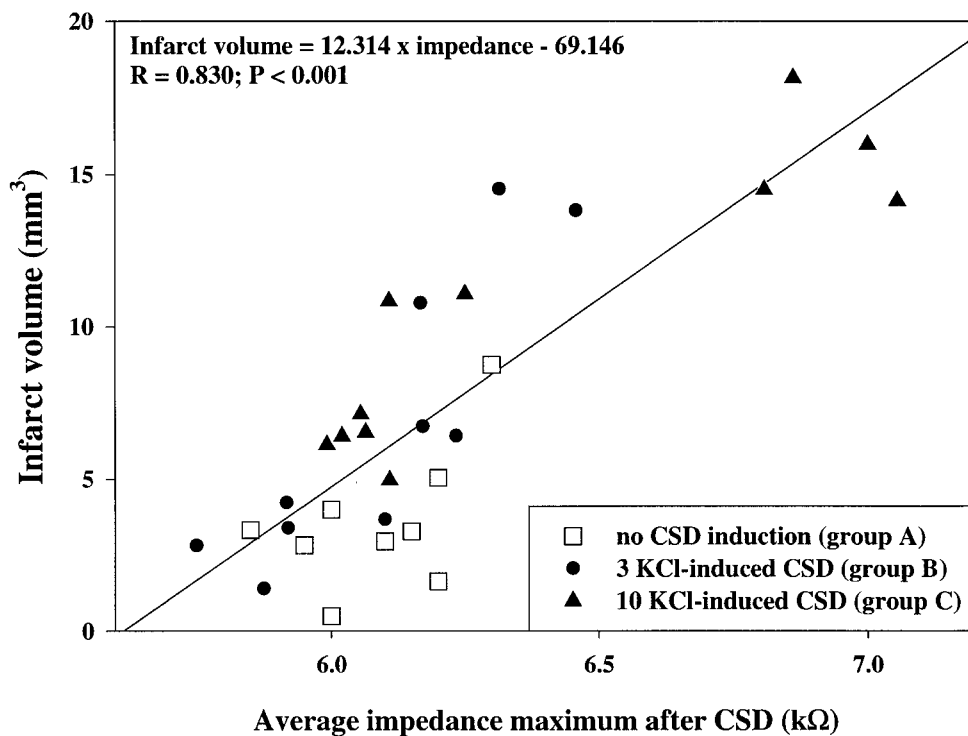


FIG. 10. Correlation of average impedance maximum due to individual CSDs (spontaneous as well as KCl induced) and infarction volumes in animals from the groups without CSD induction, with 3 KCl-induced CSDs, and with 10 KCl-induced CSDs.

infarct (Fig. 7). This does not imply that 4 spreading depression waves are sufficient to exert that effect: it is rather likely that in animals with a high initial peri-infarct depolarization frequency these events have continued during the following hours. This is underlined by the observation that 3 additionally induced CSD waves did not alter the regression line in Fig. 4. Ten induced CSD waves, on the other hand, shifted the regression line upward toward larger infarct volumes as an indication of a critical frequency at which damage from CSD increases.

The Relationship between ICBF and Brain Damage

As time passed after venous occlusion, CBF decreased in most animals (Table 1). In group C the ICBF decrease was most pronounced and statistically significant to 15.53 ± 6.51 LD units (70.8% of group A) at 75 min after occlusion. The flow reached after 75 min predicted the infarct size found after 5 days in the individual groups (Fig. 8). In those animals with flow above 15 LD units infarct volumes were smaller than in rats with lower flow values. The significance of residual flow is also illustrated in Fig. 9. Those animals had particularly large infarcts which responded with reduced ICBF increases during CSD: in those rats the reserve capacity of the microcirculatory network was apparently exhausted. Figure 9 shows also that exposure of the low-flow zone to 10 induced CSD waves may have posed an additional risk. Even in rats in which CSD could still evoke significant ICBF responses, infarction volumes found were nearly doubled compared to animals without CSD induction.

We knew before that CBF in the drainage area of the occluded veins often deteriorates with time because the thrombus grows and occludes collateral veins (23). It remains to be shown how CSD further reduces the already compromised flow in the penumbra. The example given in Fig. 4 illustrates the often observed flow decrease after CSD. Lauritzen *et al.* (13) as well as Duckrow (5) reported that CBF in healthy brain may be reduced after CSD for approx 1 h; however, they were unable to explain this hypoperfusion. In the present study, ICBF in seven rats declined suddenly following the transient CBF increase during CSD. These animals in the early phase after photothrombosis had a moderate flow reduction only, which became severe after the first CSD wave (cf. Fig. 4). Taken together our data suggest that repeated CSD can reduce blood flow in the penumbra. Further studies are required to understand the mechanisms involved.

Cell Swelling Due to CSD

Cerebral tissue impedance is determined by the intra/extracellular space ratio. Owing to the high electrical resistance of cell membranes a low-frequency

alternating current flows mainly through the extracellular space (4, 30, 31), and impedance increases if the intracellular space expands. Therefore, impedance is a reliable parameter showing the degree of cell swelling or cytotoxic brain edema. It is well established that during spreading depression the impedance increases temporarily as a consequence of the breakdown of ion gradients and, hence, cell swelling (31). Very similar although permanent and larger impedance changes are seen during anoxic depolarization. The loss of ion homeostasis during CSD and the ensuing stimulation of ion pumping are major causes of the dramatic increase of the metabolic demands after CSD. The current study demonstrates that in a penumbra situation with limited metabolic recovery at low ICBF swelling may proceed further than in healthy tissue before ion pumps can cope with it. This is evidenced by the correlation of the average impedance change seen in individual rats and the resulting infarct (Fig. 10). In our hands the impedance signal is more reproducible and correlates far better with infarct size than the DC negativity, which has also been reported to vary in size with severity of the penumbra situation and the resulting infarct (2).

CONCLUSION

The current experiments provide evidence that the two-vein occlusion model is useful to study the pathophysiology of critically perfused brain areas after vein occlusion, which turns out qualitatively similar to the arterial ischemic penumbra. Because of its widespread flow reduction, which deteriorates gradually, the model appears particularly suited to identify mediator mechanisms promoting infarct growth. Spreading depression is confirmed as such a mediator mechanism. The data suggest that a critical number of CSD waves is required to increase infarct volume. Future studies have to determine factors responsible for CSD propagation from the ischemic core into penumbra tissue.

ACKNOWLEDGMENTS

The authors thank Fatemeh Kafai for excellent secretarial assistance and Andrea Schollmayer, Michael Malzahn, and Laszlo Kopacz for their technical help and support.

REFERENCES

1. Astrup, J., B. K. Siesjö, and L. Symon. 1981. Thresholds in cerebral ischemia—The ischemic penumbra. *Stroke* **12**: 723–725.
2. Back, T., M. Ginsberg, W. D. Dietrich, and B. D. Watson. 1996. Induction of spreading depression in the ischemic hemisphere following experimental middle cerebral artery occlusion: Effect on infarct morphology. *J. Cereb. Blood Flow Metab.* **16**: 202–213.
3. Back, T., K. Kohno, and K. A. Hossmann. 1994. Cortical negative DC deflections following middle cerebral artery occlusion.

- sion and KCl-induced spreading depression: Effect on blood flow, tissue oxygenation, and electroencephalogram. *J. Cereb. Blood Flow Metab.* **14**: 12–19.
4. Baethmann, A., and A. Van Harreveld. 1973. Water and electrolyte distribution in gray matter rendered edematous with a metabolic inhibitor. *J. Neuropathol. Exp. Neurol.* **32**: 408–423.
 5. Duckrow, R. B. 1991. Regional cerebral blood flow during spreading cortical depression in conscious rats. *J. Cereb. Blood Flow Metab.* **11**: 150–154.
 6. Gill, R., P. Andiné, L. Hillered, L. Persson, and H. Hagberg. 1992. The effect of MK-801 on cortical spreading depression in the penumbral zone following ischemia in the rat. *J. Cereb. Blood Flow Metab.* **12**: 371–379.
 7. Ginsberg, M. D. 1997. Injury mechanisms in the ischemic penumbra—Approaches to neuroprotection in acute ischemic stroke. *Cerebrovasc. Dis.* **7**(Suppl. 2): 7–12.
 8. Gjedde, A., A. J. Hansen, and B. Quistorff. 1981. Blood–brain glucose transfer in spreading depression. *J. Neurochem.* **37**: 807–812.
 9. Heimann, A., T. Takeshima, G. Horstick, and O. Kempfski. 1999. Cl-esterase inhibitor reduces infarct volume after cortical vein occlusion. *Brain Res.* **838**: 210–213.
 10. Hossmann, K.-A. 1994. Viability thresholds and the penumbra of focal ischemia. *Ann. Neurol.* **36**: 557–565.
 11. Hossmann, K.-A. 1996. Perinfarct depolarizations. *Cerebrovasc. Brain Metab. Rev.* **8**: 195–208.
 12. Kempfski, O., A. Heimann, and U. Strecker. 1995. On the number of measurements necessary to assess regional cerebral blood flow by local laser Doppler recordings: A simulation study with data from 45 rabbits. *Int. J. Microcirc.* **15**: 37–42.
 13. Lauritzen, M., M. B. Jørgensen, N. H. Diemer, A. Gjedde, and A. J. Hansen. 1982. Persistent oligemia of rat cerebral cortex in the wake of spreading depression. *Ann. Neurol.* **12**: 469–474.
 14. Lauritzen, M., A. J. Hansen, and T. Wieloch. 1987. Metabolic changes with spreading depression in rat cortex. *J. Cereb. Blood Flow Metab.* **7**: S125.
 15. Leão, A. A. P. 1944. Spreading depression of activity in cerebral cortex. *J. Neurophysiol.* **7**: 359–390.
 16. Matsushima, K., M. J. Hogan, and A. M. Hakim. 1996. Cortical spreading depression protects against subsequent focal cerebral ischemia in rats. *J. Cereb. Blood Flow Metab.* **16**: 221–226.
 17. Mayevsky, A., and H. R. Weiss. 1991. Cerebral blood flow and oxygen consumption in cortical spreading depression. *J. Cereb. Blood Flow Metab.* **11**: 829–836.
 18. Mies, G., and W. Paschen. 1984. Regional change of blood flow, glucose, and ATP content determined on brain sections during a single passage of spreading depression in rat brain cortex. *Exp. Neurol.* **84**: 249–258.
 19. Mies, G., T. Iijima, and K.-A. Hossmann. 1993. Correlation between periinfarct DC shifts and ischemic neuronal damage in rat. *NeuroReport* **4**: 709–711.
 20. Nakase, H., T. Kakizaki, K. Miyamoto, K. Hiramatsu, and T. Sakaki. 1995. Use of local cerebral blood flow monitoring to predict brain damage after disturbance to the venous circulation: Cortical vein occlusion model by photochemical dye. *Neurosurgery* **37**: 280–286.
 21. Nakase, H., A. Heimann, and O. Kempfski. 1996. Local cerebral blood flow in a rat cortical vein occlusion model. *J. Cereb. Blood Flow Metab.* **16**: 720–728.
 22. Nakase, H., A. Heimann, and O. Kempfski. 1996. Alterations of regional cerebral blood flow and oxygen saturation in a rat sinus-vein thrombosis model. *Stroke* **27**: 720–728.
 23. Nakase, H., O. Kempfski, A. Heimann, T. Takeshima, and J. Tintera. 1997. Microcirculation after cerebral venous occlusions as assessed by laser Doppler scanning. *J. Neurosurg.* **87**: 307–314.
 24. Nakase, H., K. Nagata, H. Otsuka, T. Sakaki, and O. Kempfski. 1998. Local cerebral blood flow autoregulation following “asymptomatic” cerebral venous occlusion in the rat. *J. Neurosurg.* **89**: 118–124.
 25. Nedergaard, M., and J. Astrup. 1986. Infarct rim: Effect of hyperglycemia on direct current potential and [¹⁴C]2-deoxyglucose phosphorylation. *J. Cereb. Blood Flow Metab.* **6**: 607–615.
 26. Nedergaard, M., and A. J. Hansen. 1988. Spreading depression is not associated with neural injury in the normal brain. *Brain Res.* **449**: 395–398.
 27. Soehle, M., A. Heimann, and O. Kempfski. 1998. Postischemic application of lipid peroxidation inhibitor U-101033E reduces neuronal damage after global cerebral ischemia in rats. *Stroke* **29**: 1240–1247.
 28. Tehindranravelo, A., S. Evrard, M. Schaison, J.-L. Mas, D. Dormont, and M.-G. Bousser. 1992. Prospective study of cerebral sinus venous thrombosis in patients with benign intracranial hypertension. *Cerebrovasc. Dis.* **2**: 22–27.
 29. Uranishi, R., H. Nakase, T. Sakaki, and O. Kempfski. 1999. Evaluation of absolute cerebral blood flow by laser-Doppler scanning—Comparison with hydrogen clearance. *J. Vasc. Res.* **36**: 100–105.
 30. Van Harreveld, A., and S. Ochs. 1956. Cerebral impedance changes after circulatory arrest. *Am. J. Physiol.* **187**: 180–192.
 31. Van Harreveld, A. 1972. The extracellular space in the vertebrate central nervous system. Pages 447–511 in G. A. Bourne, Ed., *The Structure and Function of Nervous Tissue*. Academic Press, New York.